JOURNAL OF PROPULSION AND POWER
Vol. 14, No. 4, July–August 1998

Properties of Laminar Premixed Hydrocarbon/Air Flames at Various Pressures

M. I. Hassan,* K. T. Aung,† O. C. Kwon,‡ and G. M. Faeth§
University of Michigan, Ann Arbor, Michigan 48109-2140

Outwardly propagating spherical laminar premixed flames were experimentally and computationally used to find the sensitivities of laminar burning velocities to flame stretch, represented by Markstein numbers, and the fundamental laminar burning velocities of unstretched flames. Conditions considered included ethane, ethylene, and propane/air flames at fuel-equivalence ratios of 0.8–1.6, and pressures of 0.5–4.0 atm at normal temperatures. Predictions were limited to unstretched (plane) flames using mechanisms based on GRI-Mech, finding reasonably good agreement between measurements and predictions. An interesting experimental finding was that Markstein numbers tended to become negative over broader ranges of fuel-equivalence ratios as the pressure increased, suggesting a greater propensity toward unstable combustion because of preferential-diffusion effects at the elevated pressures of interest for most practical applications.

Nomenclature

D = mass diffusivity
K = flame stretch or the normalized rate of increase of flame surface area, Eq. (4)
Ka = Karlovitz number, KD_u/S_L^2
L = Markstein length, Eq. (1)
Ma = Markstein number, L/δ_D
P = pressure
r_f = flame radius
S_L = laminar burning velocity based on unburned gas properties
S_L' = value of S_L at largest radius observed
t = time
δ_D = characteristic flame thickness, D_u/S_L
ρ = density
ϕ = fuel-equivalence ratio

Subscripts
b = burned gas properties
max = maximum observed value
u = unburned gas properties
∞ = unstretched flame condition

Introduction

RECENT experimental and computational studies of the effects of flame stretch on laminar premixed flames in this laboratory[1–7] were extended to consider propane, ethane, and ethylene/air flames at pressures of 0.5–4.0 atm and normal temperatures (298 ± 2 K). This work was undertaken to systematically consider effects of pressure variations that are relevant to practical applications of hydrocarbon/air flames on preferential-diffusion/stretch interactions, motivated by recent findings that these interactions are very important for hydrocarbon/air flames.[1–3] Outwardly propagating spherical laminar premixed flames were considered to find the sensitivities of laminar burning velocities to flame stretch, represented by Markstein numbers, and the fundamental laminar burning velocities of unstretched flames. In addition, the new measurements were used to evaluate the C/H/O chemical reaction rate mechanism from to Frenklach et al.¶ as well as an extended version of this mechanism for propane/air and ethylene/air flames based on numerical simulations of unstretched laminar premixed flames. The following description of the study is brief, see Refs. 1–7 for more details about experimental and computational methods.

Present experiments and computational results were analyzed to find flame/stretch interactions caused by preferential-diffusion effects in the same way as earlier studies of outwardly propagating spherical laminar premixed flames in this laboratory.[1–7] This involves a conservative selection of flame conditions so that problems of flame thickness variations, curvature, and unsteadiness caused by laminar burning velocity variations with flame radius were minimized when flame properties were interpreted by limiting observations of conditions where $\delta_D/r_f < 0.02$.[2,4] Effects of stretch on laminar burning velocities were correlated according to an early proposal of Markstein,[8] after a later extension at the limit of small stretch by Clavin[9]:

$$S_L = S_{L\infty} - LK \tag{1}$$

To account for large values of stretch during the present study, Eq. (1) was extended so that the flame response to stretch was represented by the characteristic length and time scales of stretched flames, δ_D and δ_D/S_L, rather than corresponding scales for unstretched flames, to yield[1–7]

$$S_{L\infty}/S_L = 1 + MaKa \tag{2}$$

Past observations generally show that Ma is independent of Ka when $\delta_D/r_f \ll 1$, which provides a concise summary of flame/stretch interactions as a single Markstein number for each reactant mixture and pressure.[1–7] The small stretch limit

Received July 30, 1997; revision received Jan. 26, 1998; accepted for publication Jan. 28, 1998.

*Visiting Scholar, Department of Aerospace Engineering; currently, Lecturer, Mechanical Power Department, Helwan University, Cairo, Egypt.
†Graduate Student Research Assistant, Department of Aerospace Engineering; currently, Post Doctoral Fellow, School of Aerospace Engineering, Georgia Institute of Technology, Atlanta, GA 30332.
‡Graduate Student Research Assistant, Department of Aerospace Engineering.
§Professor, Department of Aerospace Engineering. Fellow AIAA.

¶Data may be accessed online at http://www.me.berkeley.edu/grimech (1997).

of Eq. (2) is also of interest; this expression can be found from Eq. (2), as follows[4]:

$$S_L/S_{L\infty} = 1 - Ma_\infty Ka_\infty, \qquad Ka_\infty << 1 \tag{3}$$

Notably, Eq. (3) is identical to the findings of classical theories at the limit of small stretch.[9]

The present characterization of premixed flame/stretch interactions is only one of many possibilities, but it has several advantages pending the development of generally accepted methods to treat these interactions outside the small stretch limit, as follows: data reduction does not involve flame structure models that are difficult to fully define and are likely to be revised as more information about flame/stretch interactions is developed, the characterization is concise, this facilitates use of the results by others, the positive and negative ranges of Ma provide a direct indication of stable and unstable flame surface conditions with respect to effects of preferential diffusion, and the results can be readily transformed to provide direct comparisons with other characterizations of premixed flame/stretch interactions. Nevertheless, the present approach has only been applied to outwardly propagating spherical laminar premixed flames when $\delta_D/r_f << 1$ and effects of ignition disturbances and radiation are small. The limitations of this approach for more general conditions are not known so that direct use of present Ma to characterize the effects of stretch in other circumstances should be approached with caution.

The properties of the laminar burning velocities of propane, ethane, and ethylene/air flames at normal temperature and pressure (NTP) have been considered during several previous experimental investigations, see Refs. 10–21 and references therein. The earliest studies[10–16] did not consider effects of flame stretch on laminar burning velocities that are now known to be significant for hydrocarbons[2]; therefore, interpretation of these results is problematic. Subsequently, Law and co-workers[17–19] measured the laminar burning velocities of some hydrocarbon/air mixtures using the counterflow twin-flame technique, while extrapolating measurements at finite stretch rates to estimate fundamental unstretched laminar burning velocities; however, the flame response to stretch was not quantified. Taylor[20] studied outwardly propagating spherical flames similar to the present investigation while using a different extrapolation procedure to estimate effects of stretch on the laminar burning velocities for methane, ethanol, ethylene, and propane/air flames; however, effects of flame response to stretch were limited to small values of stretch, whereas effects of pressure were not quantified.

Past work in this laboratory[1–7] for hydrocarbon-fueled premixed flames includes measurements of flame/stretch interactions for methane, ethane, ethylene, and propane/air flames at normal temperature and pressure (NTP).[2,3] This was followed by consideration of methane/air flames, both experimentally and computationally, for pressures of 0.5–4.0 atm at normal temperature.[7] The latter study suggested reasonably good capabilities for predicting the flame/stretch response as Markstein numbers, and the fundamental laminar burning velocities of unstretched flames based on the chemical kinetic mechanisms of Frenklach et al. These results also suggested a potentially significant trend that methane/air flames exhibited progressively increased tendencies toward flame instability because of preferential-diffusion effects with increasing pressure. Thus, it is of interest to see whether flames of other relatively light hydrocarbons can be modeled using these kinetics with similar success, and whether these hydrocarbons also exhibit a tendency toward increased preferential-diffusion instabilities with increasing pressure.

In view of the current status of understanding flame/stretch interactions caused by preferential-diffusion effects for laminar premixed hydrocarbon/air flames, the objectives of the present study were as follows.

1) To measure the properties of outwardly propagating spherical laminar premixed flames of propane, ethane, and ethylene/air mixtures for various fuel-equivalence ratios, pressures, and degrees of stretch at normal temperature, within the allowable range of conditions using present data reduction methods.

2) To reduce the measurements to find corresponding Markstein numbers and unstretched laminar burning velocities.

3) To complete numerical simulations of the corresponding unstretched laminar flames using contemporary detailed chemical reaction mechanisms.

4) To compare measurements and predictions of unstretched laminar burning velocities with each other and with earlier results in the literature.

The present discussion begins with descriptions of experimental and computational methods. Results are then considered by treating flame response to stretch, unstretched laminar burning velocities, and flame structure. The present description of experimental and computational methods is brief, see Refs. 1–7 for more details.

Experimental Methods

The experiments were carried out in the spherical windowed chamber used for recent studies of laminar premixed-flame/stretch interactions in this laboratory.[4–7] The reactant mixture was prepared in a separate chamber by adding gases at appropriate partial pressures, allowed to stand overnight, and then checked using gas chromatography before use. The combustible mixture was spark-ignited at the center of the chamber, using spark energies near minimum ignition energies to control ignition disturbances. Motion picture shadowgraphy was used to observe the motion of the flame surface and the possible development of wrinkled surfaces caused by the effects of instabilities. Measurements were limited to flames having diameters less than 60 mm, which implies pressure increases less than 0.4% of the initial pressure during the period of propagation. Finally, earlier measurements showed that the effects of burned gas motion and wall disturbances are small for the present test arrangement.[1]

Measurements were limited to $\delta_D/r_f \leq 2\%$, so that effects of curvature and transient phenomena associated with flame thicknesses were small.[2] In addition, estimates showed that radiative heat losses were smaller than 5% of the rate of chemical energy release within the flames, implying small effects of radiation on flame properties as well. Finally, minimum flame radii were greater than 5 mm to avoid ignition disturbances and satisfy the minimum δ_D/r_f criterion mentioned earlier. For these conditions the laminar burning velocity and flame stretch are given by[24]

$$S_L = \left(\frac{\rho_b}{\rho_u}\right)\frac{dr_f}{dt}, \qquad K = \left(\frac{2}{r_f}\right)\frac{dr_f}{dt} \tag{4}$$

Similar to past work,[1–7] the density ratio needed in Eq. (4) was computed assuming adiabatic combustion at constant pressure with the reactant temperature equal to the initial temperature and with the same fuel-equivalence ratio, i.e., the same elemental composition, in the unburned and burned gases. These computations were carried out using the adiabatic flame algorithms of Gordon and McBride[23] and Reynolds,[24] both yielding the same results. It should be noted, however, that use of the unstretched flame density ratio in this manner is a convention that ignores preferential-diffusion effects that modify the local mixture fraction and thermal energy transport and, thus, the density ratio of stretched flames. This convention is convenient, however, because a single density ratio is used to relate flame speeds and laminar burning velocities for all values of flame stretch, which avoids current uncertainties about the effects of stretch on flame jump conditions. The present approach also corresponds to methods used during past studies

of preferential-diffusion/stretch interactions,[1–7,17–20] which simplifies comparison of various determinations of flame properties. This approach also retrieves the correct displacement velocity of the flame, dr_f/dt. Nevertheless, given successful evaluation of methods of predicting the structure of stretched propane, ethane, and ethylene/air flames, density ratios should be computed for various degrees of stretch so that present measurements could be used more accurately to estimate the laminar burning velocities and the mass burning rates of these flames.

Final results were obtained by averaging the measurements of 4–6 tests at each condition. Methods of estimating experimental uncertainties are discussed elsewhere[4]; the present uncertainties (95% confidence) are as follows: S_L is less than 9%, Ka is less than 21%, S_{L_z} is less than 12%, and Ma is less than 25% for $|Ma| > 1$, with uncertainties of $|Ma|$ increasing inversely proportional to $|Ma|$ for values less than unity.

The experimental conditions and major results (D_u, ρ_u/ρ_b, S_{L_z}, Ka_{max}, and Ma, where results to be discussed later show that Ma is constant for $Ka \leq Ka_{max}$) are summarized in Tables 1–3 as a function of pressure for propane, ethane, and ethylene/air flames, respectively. The total test range includes pressures of 0.5–4.0 atm and fuel-equivalence ratios of 0.8–1.6. It should be noted that some entries of Tables 1–3 are provided for information purposes only because they involve

Table 1 Summary of test conditions[a]

ϕ	0.8	0.9	1.0	1.1	1.2	1.3	1.4	1.6
P = 0.5 atm								
ρ_u/ρ_b	7.02	7.52	7.88	8.01	7.97	7.87	7.70	7.48
S_{L_z}, mm/s	370	380	430	450	410	380	350	170
Ka_{max}	0.20	0.20	0.20	0.20	0.20	0.15	0.10	0.20
Ma	5.10	3.10	2.20	1.30	0.00	0.40	−0.50	−2.20
P = 1.0 atm								
ρ_u/ρ_b	7.04	7.56	7.93	8.06	7.99	7.87	7.75	7.48
S_{L_z}, mm/s	290	320	400	400	390	350	270	120
Ka_{max}	0.10	0.15	0.10	0.10	0.10	0.10	0.10	0.10
Ma	3.60	2.50	2.40	1.80	0.65	0.50	−1.60	−3.80
P = 2.0 atm								
ρ_u/ρ_b	7.05	7.58	7.98	8.06	8.00	7.88	7.75	——
S_{L_z}, mm/s	250	280	350	330	340	240	180	——
Ka_{max}	0.05	0.05	0.05	0.04	0.03	0.05	0.05	——
Ma	−3.60	−4.50	−4.50	−5.00	−6.10	−6.20	−7.90	——
P = 3.0 atm								
ρ_u/ρ_b	7.05	7.60	8.01	8.06	8.01	7.88	7.75	7.49
S_{L_z}, mm/s	240	260	300	300	290	200	160	70
Ka_{max}	0.03	0.04	0.03	0.03	0.03	0.04	0.04	0.06
Ma	−3.80	−4.90	−6.40	−8.70	−8.70	−9.60	−10.10	−9.80
P = 4.0 atm								
ρ_u/ρ_b	7.05	7.58	8.01	8.06	8.00	7.88	7.75	7.49
S_{L_z}, mm/s	220	250	300	290	250	220	120	60
Ka_{max}	0.03	0.03	0.03	0.03	0.02	0.03	0.03	0.03
Ma	−10.70	−10.20	−10.70	−10.10	−12.70	−10.90	−11.30	−13.50

[a] C_2H_8/air flames at 298 K (D_u = 11.5/P mm^2/s).

Table 2 Summary of test conditions[a]

ϕ	0.8	0.9	1.0	1.1	1.2	1.4	1.6
P = 0.5 atm							
ρ_u/ρ_b	6.93	7.41	7.76	7.88	7.82	7.57	7.29
S_{L_z}, mm/s	320[b]	430	450	460	460	360	240
Ka_{max}	0.30	0.25	0.25	0.25	0.20	0.30	0.40
Ma	1.10	1.00	1.00	1.15	0.40	0.30	0.25
P = 1.0 atm							
ρ_u/ρ_b	6.94	7.44	7.81	7.91	7.83	7.57	7.30
S_{L_z}, mm/s	270[b]	400	420	430	410	340	180
Ka_{max}	0.20	0.15	0.15	0.15	0.10	0.20	0.20
Ma	3.60	1.40	2.00	1.90	1.30	1.15	0.00
P = 2.0 atm							
ρ_u/ρ_b	6.95	7.47	7.86	7.94	7.84	7.58	7.30
S_{L_z}, mm/s	230[b]	340	370	370	380	250	120
Ka_{max}	0.10	0.05	0.05	0.05	0.05	0.05	0.08
Ma	−1.90	−3.00	−4.00	−4.10	−5.00	−6.00	−7.00
P = 3.0 atm							
ρ_u/ρ_b	6.96	7.49	7.89	7.96	7.85	7.58	7.30
S_{L_z}, mm/s	240[b]	310	360	340	340	210	100
Ka_{max}	0.04	0.03	0.03	0.04	0.04	0.05	0.07
Ma	−5.75	−6.00	−6.30	−7.70	−7.80	−8.10	−8.80
P = 4.0 atm							
ρ_u/ρ_b	6.96	7.49	7.90	7.96	7.85	7.58	7.30
S_{L_z}, mm/s	220[b]	280	310	320	290	170	95
Ka_{max}	0.04	0.03	0.03	0.03	0.03	0.04	0.05
Ma	−7.60	−8.49	−8.20	−9.10	−10.60	−11.50	−10.00

[a] C_2H_6/air flames at 298 K (D_u = 14.6/P mm^2/s).
[b] Provisional results because $\delta_D/r_f > 0.02$ for a portion of the database.

Table 3 Summary of test conditions[a]

ϕ	0.8	0.9	1.0	1.1	1.2	1.4	1.6
P = 0.5 atm							
ρ_u/ρ_b	7.34	7.79	8.10	−8.28	8.33	8.24	8.06
$S_{L\infty}$, mm/s	530[b]	610	690	710	690	600	380
Ka_{max}	0.20	0.20	0.15	0.15	0.15	0.15	0.30
Ma	2.20	1.60	1.40	1.60	0.90	0.70	0.10
P = 1.0 atm							
ρ_u/ρ_b	7.37	7.84	8.17	8.35	8.38	8.26	8.07
$S_{L\infty}$, mm/s	490[b]	590	650	680	650	580	330
Ka_{max}	0.15	0.10	0.10	0.10	0.10	0.10	0.20
Ma	2.40	1.50	2.10	2.20	1.00	1.50	−0.05
P = 2.0 atm							
ρ_u/ρ_b	7.39	7.89	8.24	8.40	8.41	8.27	8.08
$S_{L\infty}$, mm/s	440[b]	520	560	580	600	450	250
Ka_{max}	0.03	0.03	0.03	0.03	0.03	0.04	0.05
Ma	−1.45	−0.90	−0.80	−1.40	−0.80	−1.20	−1.40
P = 3.0 atm							
ρ_u/ρ_b	7.40	7.91	8.27	8.44	8.43	8.28	8.08
$S_{L\infty}$, mm/s	410[b]	470	550	540	530	390	220
Ka_{max}	0.05	0.05	0.03	0.04	0.04	0.05	0.10
Ma	−4.90	−6.80	−4.90	−5.90	−6.60	−6.70	−8.10
P = 4.0 atm							
ρ_u/ρ_b	7.41	7.92	8.30	8.46	8.44	8.28	8.08
$S_{L\infty}$, mm/s	390[b]	450	510	530	470	350	180
Ka_{max}	0.03	0.03	0.02	0.02	0.02	0.02	0.03
Ma	−4.00	−6.00	−6.00	−5.50	−8.50	−8.80	−9.60

[a] C_2H_4/air flames at 298 K (D_u = 15.8/P mm^2/s).
[b] Provisional results because $\delta_D/r_f > 0.02$ for a portion of the database.

values of δ_D/r_f outside the allowable range. Finally, effects of buoyancy were found to be small over the present test range.

Computational Methods

Because of the extensive detailed reaction mechanisms of propane, ethane, and ethylene/air flames, computation times needed to simulate outwardly propagating flames to find Markstein numbers, similar to past work for some relatively simplified flame systems,[4–7] were not feasible. Thus, present numerical simulations were limited to unstretched (plane) flames, and were carried out using the steady, one-dimensional laminar premixed flame computer code PREMIX.[25–29] Thermochemical and transport properties for these computations were found from Kee et al.,[25–27] except for the thermochemical properties of those species given by Frenklach et al. All properties were checked against original sources. The present calculations were carried out using the mixture-averaged multicomponent transport approximation plus thermal diffusion, while ignoring the Dufour effect, justified by earlier evaluations of transport approximations.[4–6]

The detailed reaction mechanisms of C/H/O/N-based flames have received a great deal of attention.[30–34] To control computer time and costs, only representative recent chemical reaction mechanisms by Frenklach et al. (GRI-Mech 2.1) as extended for C_3 kinetics, and an earlier approach by Egolfopoulos et al.,[17] were considered during the present study. Numerical accuracy was similar to past work,[4–7] with calculations for various grid spacings suggesting numerical accuracy of the computations of unstretched laminar burning velocities within 1%.

The chemical reaction mechanism of Frenklach et al. involves 32 species and 175 reversible reactions (not counting the range of third-body collision efficiencies). The chemical reaction mechanism extended for C_3 kinetics involves 39 species and 222 reversible reactions (not counting the range of third-body collision efficiencies). The backward rates of reaction were found from chemical equilibrium considerations using the CHEMKIN package,[27] unless the mechanism provided an alternative formulation. The full reaction mechanism of Frenklach et al. was used for ethane/air and ethylene/air flames. The extended version of this mechanism was used for propane/air and ethylene/air flames.

Results and Discussion

Flame Response to Stretch

Values of $S_{L\infty}$ were found from Eq. (2) by plotting S_L as a function of Ka. Similar to past work,[1–7] this yielded linear plots so that extrapolation to $Ka = 0$ gave $S_{L\infty}$, as summarized in Tables 1–3. Then given $S_{L\infty}$, plots of $S_{L\infty}/S_L$ as a function of Ka could be constructed for a given reactant mixture and pressure, as suggested by Eq. (2). Typical plots of this type are illustrated in Figs. 1 and 2 for propane/air mixtures at pressures of 0.5 and 4.0 atm, respectively, and in Figs. 3 and 4 for ethane/air and ethylene/air mixtures at pressures of 0.5 and 4.0 atm, respectively. Results at conditions that are stable (unstable) with respect to preferential-diffusion effects, corresponding to $Ma > 0$ ($Ma < 0$), are indicated by opened (darkened) symbols on these plots.

The measurements illustrated in Figs. 1–4 illustrate the linear relationship between $S_{L\infty}/S_L$ and Ka that was exploited to find $S_{L\infty}$ similar to past work.[1–7] Thus, the slope of each plot, which is equal to the Markstein number according to Eq. (2), is independent of Ka over the range of the present measurements. These ranges involve $Ka < 0.2$ for propane/air flames, and <0.4 for ethane- and ethylene/air flames, which are not close to extinction conditions (where Ka would be on the order of unity[35]), where the response of the flames to variations of Ka is likely to change. In contrast to earlier findings for hydrogen/air, CO/H_2/air and methane/air flames,[4–7] the responses of propane, ethane, and ethylene/air flames to stretch tend to yield stable flames at lean conditions and unstable flames at rich conditions. Flame/stretch interactions are substantial in these fuels, affecting the laminar burning velocities by factors in the 0.6–1.5 range, even for the relatively modest ranges of flame stretch considered during the present investigation ($Ka < 0.4$). Another interesting general trend seen for all of these hydrocarbons is the progressively increased range of fuel-equivalence ratios, where unstable behavior is observed with increasing pressure; notably, this trend was also evident for methane/air flames.[7]

Present experimentally determined Markstein numbers are independent of Ka for $Ka < Ka_{max}$ and are summarized in Tables 1–3. Markstein numbers for propane/air flames are plotted as functions of fuel-equivalence ratios at various pressures in

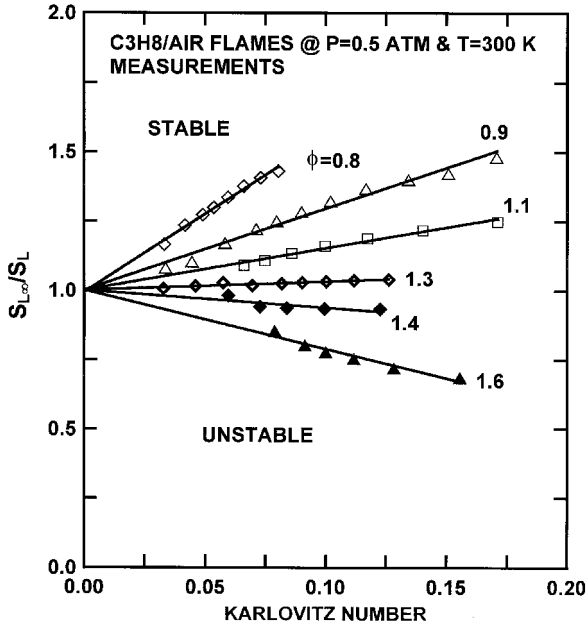

Fig. 1 Measured laminar burning velocities as a function of Karlovitz number and fuel-equivalence ratio for propane/air flames at a pressure of 0.5 atm.

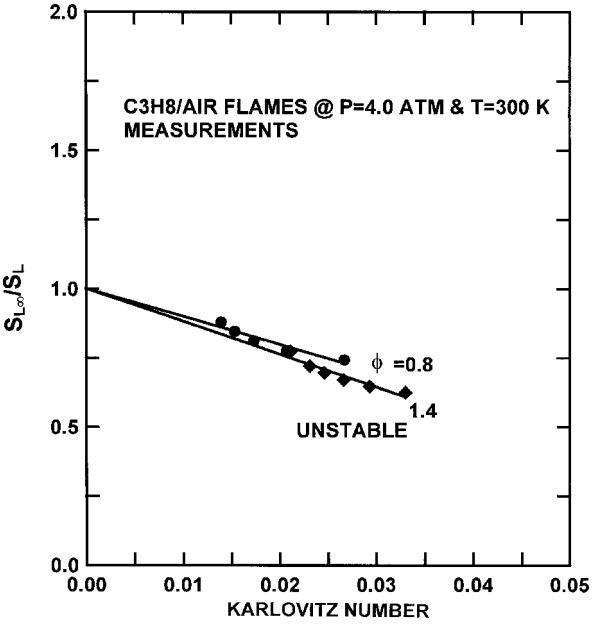

Fig. 2 Measured laminar burning velocities as a function of Karlovitz number and fuel-equivalence ratio for propane/air flames at a pressure of 4.0 atm.

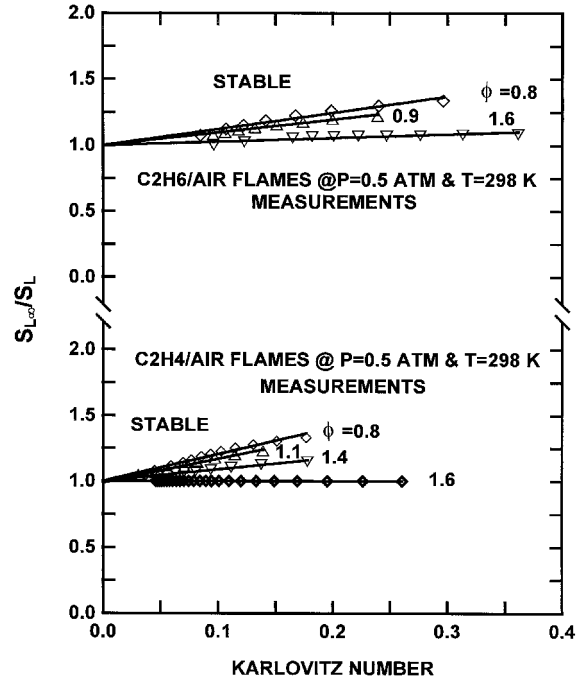

Fig. 3 Measured laminar burning velocities as a function of Karlovitz number and fuel-equivalence ratio for ethane and ethylene/air flames at a pressure of 0.5 atm.

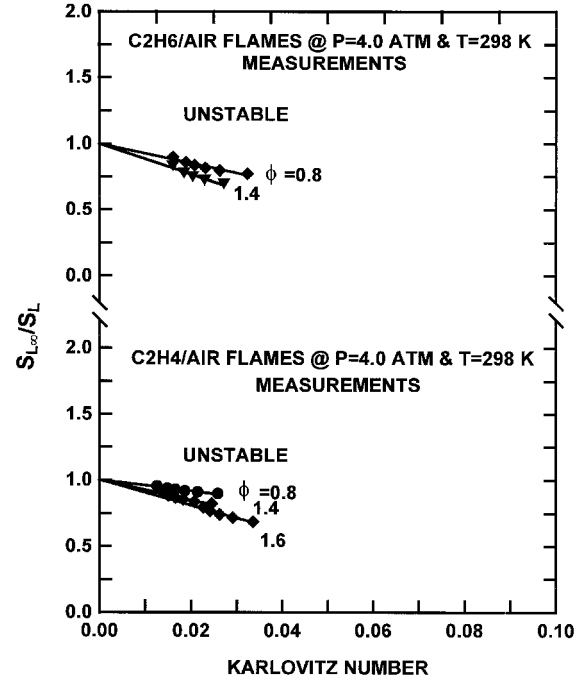

Fig. 4 Measured laminar burning velocities as a function of Karlovitz number and fuel-equivalence ratio for ethane and ethylene/air flames at a pressure of 4.0 atm.

Fig. 5. These results include the measurements of Tseng et al.[2] and Taylor[20] at atmospheric pressure and the present measurements at pressures of 0.5–4.0 atm. Present measurements of Markstein numbers are independent of *Ka* and can be compared with those of Taylor found at the limit of small stretch. All three sets of measurements at atmospheric pressure are seen to agree well within experimental uncertainties. Measurements of *Ma* are positive for nearly the full range of fuel-equivalence ratios at 0.5 atm, only approaching unstable conditions at $\phi = 1.6$, which implies that these flames mainly are preferential-diffusion stable. On the other hand, measurements of *Ma* are strongly negative (in the -8 to -12 range) over the whole range of fuel-equivalence ratios at a pressure of 4.0 atm. The reversed behavior of propane/air flames compared to hydrogen, wet carbon monoxide, and methane/air flames (generally stable at lean as opposed to rich conditions) is expected because of the large differences between the mass diffusivities of these fuels and air. For propane/air flames, the mass diffusivity of the oxidizer is larger than the mass diffusivity of the fuel; therefore, oxygen will diffuse faster to the flame front when the flame is stretched, which reduces the local fuel-to-air ratio. At lean conditions, decreasing the fuel-to-air ratio causes laminar burning velocities to decrease as well, which implies stable preferential-diffusion conditions. On the other hand, at the rich conditions, reducing the fuel-to-air ratio causes the laminar burning velocities to increase, which im-

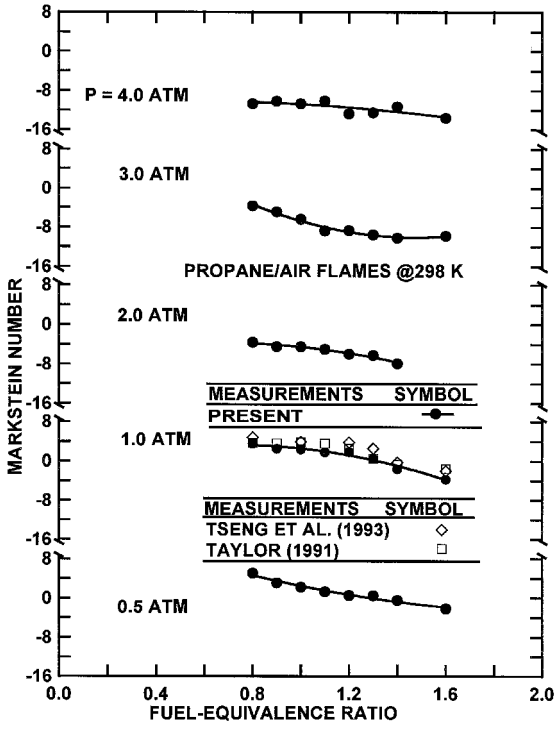

Fig. 5 Measured Markstein numbers as a function of fuel-equivalence ratio for propane/air flames at various pressures. Measurements of Tseng et al.,[2] Taylor,[20] and the present investigation.

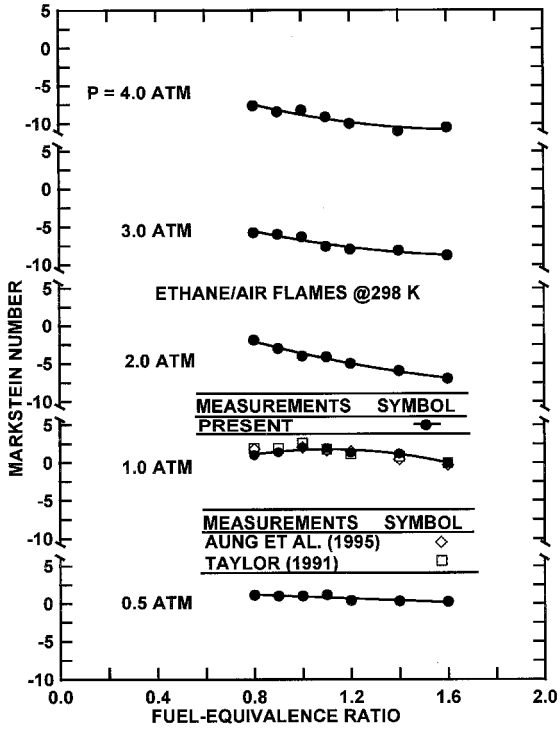

Fig. 6 Measured Markstein numbers as a function of fuel-equivalence ratio for ethane/air flames at various pressures. Measurements of Aung et al.,[3] Taylor,[20] and the present investigation.

plies unstable preferential-diffusion conditions. In addition, the light radicals are crucial to oxidation processes in all of these flames and their preferential-diffusion behavior might be expected to increase the sensitivity to stretch as well.

The Markstein numbers of ethane and ethylene/air flames are plotted as functions of the fuel-equivalence ratio for various initial pressures in Figs. 6 and 7. These plots show the

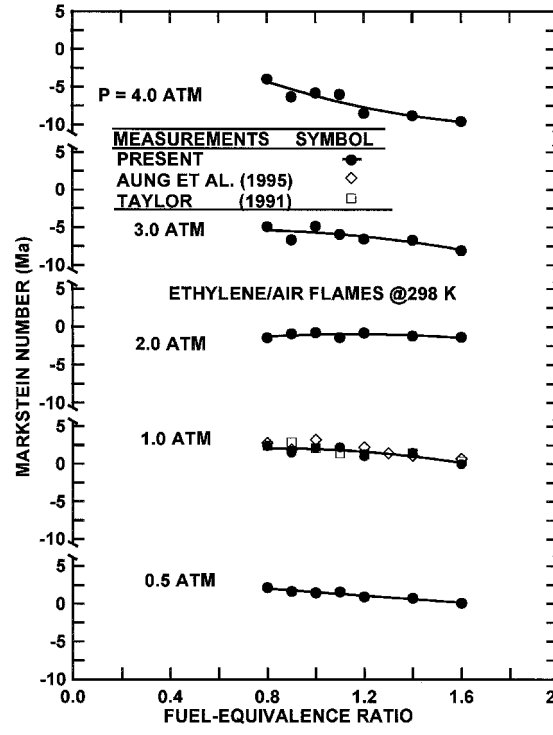

Fig. 7 Measured Markstein numbers as a function of fuel-equivalence ratio for ethylene/air flames at various pressures. Measurements of Aung et al.,[3] Taylor,[20] and the present investigation.

measurements of Aung et al.[3] and Taylor[20] at atmospheric pressure as well as the present results for pressures in the 0.5–4.0 atm range. The measurements of Aung et al. and Taylor agree well within experimental uncertainties with the present measurements. Measurements for *Ma* for ethane and ethylene/air flames exhibit small positive values at all fuel-equivalence ratios for pressures up to 1.0 atm, which implies that the low-pressure ethane and ethylene/air flames are not strongly affected by preferential-diffusion phenomena. On the other hand, the measurements at high pressures (over 1.0 atm) show that ethane and ethylene/air flames exhibit negative values of *Ma* over the whole range of fuel-equivalence ratios, which is quite similar to the propane/air flames.

Taken together, the Markstein numbers of propane, ethane, and ethylene/air flames progressively become more negative as the pressure is increased and generally also tend to decrease as the fuel-equivalence ratio is increased. This behavior yields broad ranges of large negative values of *Ma* at the elevated pressures of interest for many practical applications. This behavior implies strong capabilities to enhance the distortion of flame surfaces by turbulence at elevated pressures that should be considered by models of turbulent combustion processes. Finally, this high-pressure behavior cannot be explained by simple preferential-diffusion arguments associated with the modification of fuel-equivalence ratios at the flame sheet. A more promising explanation involves preferential-diffusion of reaction intermediates such as light radical species at high pressures, where radical concentrations in the reaction zone become small because of the increased effectiveness of radical recombination reactions. The resulting increase of radical concentrations because of the effects of preferential diffusion interacting with flame stretch would then cause a corresponding increase of the laminar burning velocity, owing to the well-known relationship between radical concentrations and laminar burning velocities discussed by Padley and Sugden.[36]

Unstretched Laminar Burning Velocities

Present measurements of unstretched laminar burning velocities are summarized in Tables 1–3. Both measured and pre-

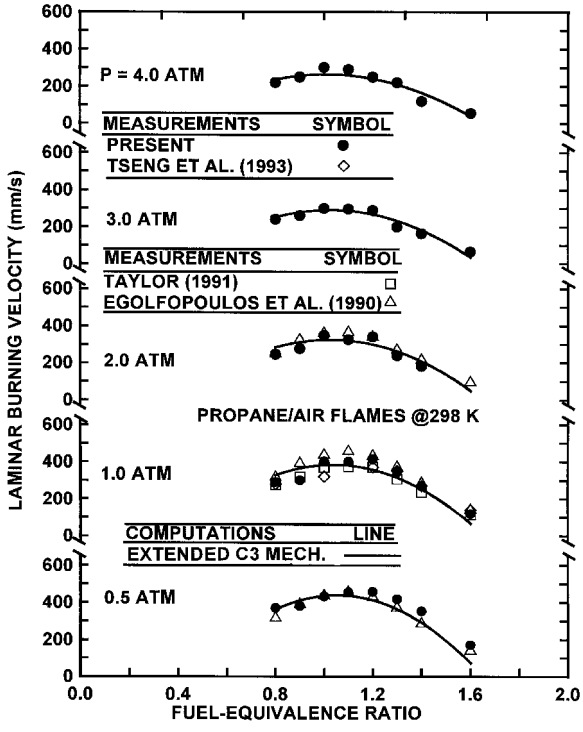

Fig. 8 Measured and predicted unstretched laminar burning velocities as a function of fuel-equivalence ratio for propane/air flames at various pressures. Measurements of Tseng et al.,[2] Taylor,[20] Egolfopoulos et al.[17] and the present investigation.

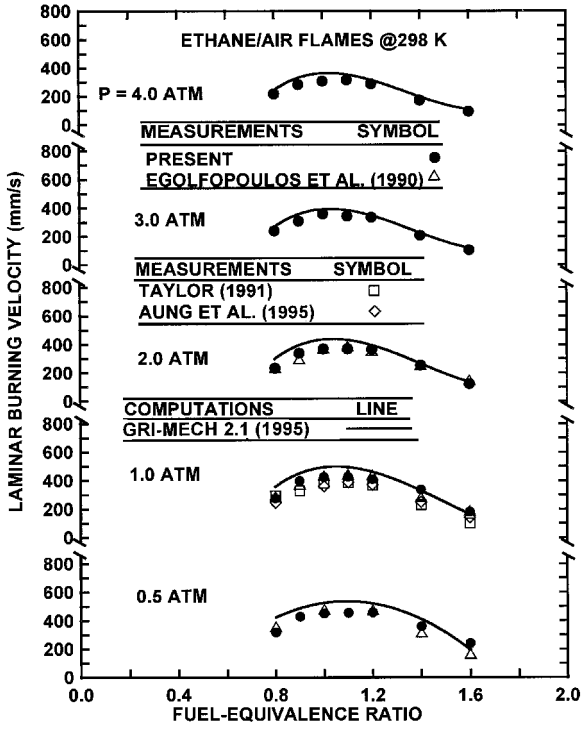

Fig. 9 Measured and predicted unstretched laminar burning velocities as a function of fuel-equivalence ratio for ethane/air flames at various pressures. Measurements of Aung et al.,[3] Taylor,[20] Egolfopoulos et al.,[17] and the present investigation; predictions based on the kinetics of GRI-Mech 2.1.

dicted unstretched laminar burning velocities for propane, ethane, and ethylene/air flames are plotted as a function of the fuel-equivalence ratio for various pressures in Figs. 8–10, respectively. Measurements illustrated in these figures include those of Aung et al. and Taylor at atmospheric pressure, those

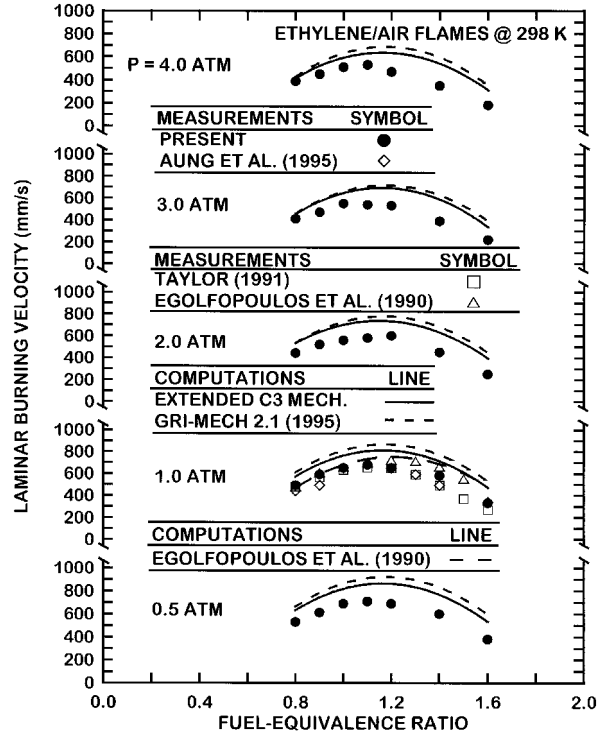

Fig. 10 Measured and predicted unstretched laminar burning velocities as a function of fuel-equivalence ratio for ethylene/air flames at various pressures. Measurements of Aung et al.,[3] Taylor,[20] Egolfopoulos et al.,[17] and the present investigation; predictions based on GRI-Mech 2.1[8] and Egolfopoulos et al.[17]

at pressures of 0.5–2.0 atm, and those of the present investigation at pressures of 0.5–4.0 atm. It is evident that the various stretch-corrected measurements agree with each other well within present experimental uncertainties even though methods of finding unstretched laminar burning velocities differ for the three studies.

The predicted unstretched laminar burning velocities illustrated in Figs. 8–10 involve the GRI-Mech 2.1 mechanism of Frenklach et al. for ethane and ethylene/air flames, and the extension of GRI-Mech 2.1 to treat propane/air and ethylene/air flames. The comparison between measurements and predictions for the propane and ethane/air flames is seen to be excellent over the test range, well within present experimental uncertainties. The comparison between measurements and predictions is not as good for ethylene/air flames, however, with predictions generally 20–30% greater than the measurements at fuel-rich conditions. At atmospheric pressure, the mechanism of Egolfopoulos et al.[17] yields excellent agreement with their measurements over the full range of fuel-equivalence ratios, although these results still are significantly larger than the measurements of Taylor, Aung et al., and the present investigation at fuel-rich conditions. The newer mechanism allowing for C_3 kinetics, however, yields results comparable to GRI-mech, which is not particularly satisfactory. Thus, additional study of ethylene/air flames is needed to resolve the differences among the various predicted and measured unstretched laminar burning velocities.

Flame Structure

As just noted, present measurements and predictions of the unstretched laminar burning velocities of unstretched ethane/air and propane/air flames generally agree within experimental uncertainties; therefore, use of the predictions to provide information about effects of pressure on the flame structure is justified to gain a better understanding of the effects of initial pressures on species concentrations within the flame and, thus, flame surface instabilities. This is done in the following for

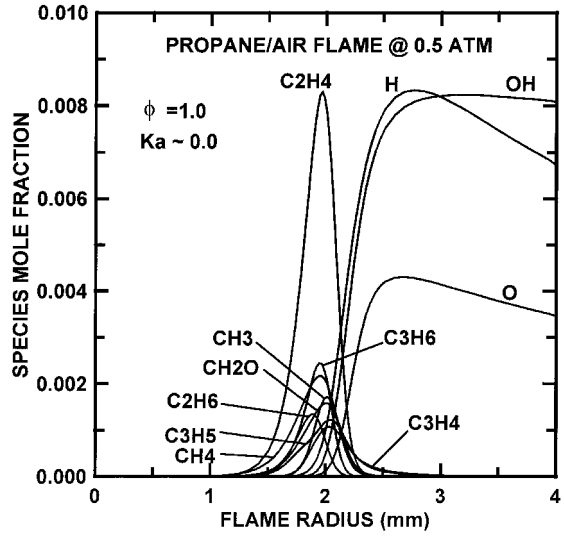

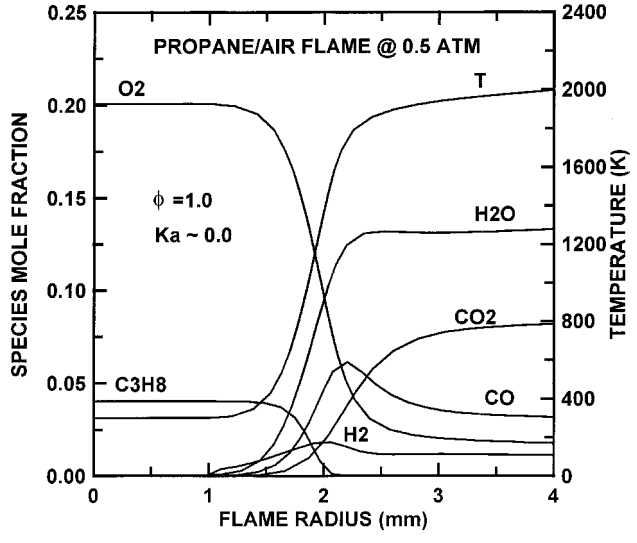

Fig. 11 Predicted structure of an unstretched (Ka = 0) propane/air flame at normal temperature and a pressure of 0.5 atm (ϕ = 1.0).

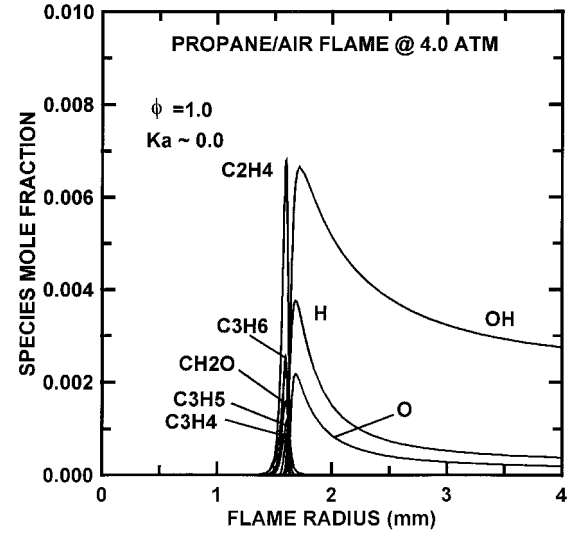

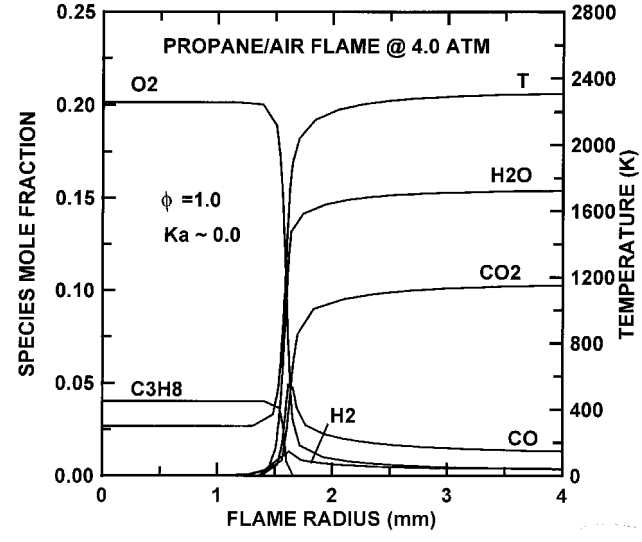

Fig. 12 Predicted structure of an unstretched (Ka = 0) propane/air flame at normal temperature and a pressure of 4.0 atm (ϕ = 1.0).

propane/air flames using the chemical reaction mechanism and the unstretched flame simulation code (PREMIX) of Kee and coworkers.[25–29]

The structure of unstretched propane/air flames at stoichiometric conditions is illustrated in Figs. 11 and 12 for pressures of 0.5 and 4.0 atm, respectively. These calculations were carried out for an unstretched (plane) flame; thus, the origin of the radial coordinate system in these figures was arbitrary. Comparing Figs. 11 and 12, it can be seen that the increase in pressure increases the flame temperatures because of reduced dissociation (note the corresponding increase of the stable combustion produces CO_2 and H_2O). Nevertheless, in spite of increased reaction zone temperatures, increased rates of the three-body recombination reactions at elevated pressures cause significant reductions of all radical concentrations in the high-pressure flame. Through the well-known proportionality between radical concentrations in the reaction zone and laminar burning velocities,[36] the reduced radical concentrations in the reaction zone are responsible for the significant reduction of laminar burning velocities with increasing pressure seen in Fig. 8 for propane/air flames. This deficiency of highly diffusive light radials at high pressures also provides a potential explanation for increased effects of preferential-diffusion instability at high pressures; however, proof of this effect will require detailed numerical simulations of stretched propane, ethane, and ethylene/air flames, similar to recent results for methane/air flames.[7]

Conclusions

The effects of pressure variations on the preferential-diffusion/stretch interactions of hydrocarbon/air flames at normal temperature were studied experimentally and computationally. The hydrocarbon fuels considered were propane, ethane, and ethylene. The measurements involved the outwardly propagating spherical laminar premixed flame configuration. The computations were limited to the unstretched (plane) laminar premixed flame configuration. The test conditions involved fuel-equivalence ratios in the range 0.8–1.6, pressures in the range 0.5–4.0 atm, Karlovitz numbers in the 0–0.4 range and laminar burning velocities in the range 220–450 mm/s for propane/air and ethylene/air flames and 390–710 mm/s for ethylene/air flames, respectively. The corresponding Markstein numbers were in the −13.5 to 5.1 range for these test conditions. The major conclusions of study are as follows:

1) Effects of flame/stretch interactions for the measurements could be correlated according to $S_{L^\infty}/S_L = 1 + MaKa$, where S_{L^∞}/S_L varies linearly with Ka, yielding Markstein numbers that were only functions of reactant composition and pressure for

the present range of Karlovitz numbers ($Ka < 0.4$), similar to past work in this laboratory.

2) Effects of flame stretch on laminar burning velocities were substantial, even though present flames did not approach quenching conditions, yielding values of S_{L^2}/S_L as follows: 0.6–2.0 for propane/air flames, 0.4–1.3 for ethane/air flames, and 0.2–1.4 for ethylene/air flames. Corresponding ranges of Markstein numbers were as follows: −13.5 to 5.1 for propane/air flames, −11.5 to 2.0 for ethane/air flames, and −9.6 to 2.4 for ethylene/air flames.

3) At modest pressures (0.5–1.0 atm), the present flames exhibited either stable preferential-diffusion behavior at lean conditions (propane/air flames) or near-neutral behavior everywhere (ethane and ethylene/air flames), which agrees with classical ideas about the effects of preferential-diffusion of reactant species on flame stability. On the other hand, the flame stability mechanism changes at elevated pressures, where values of Markstein numbers tend to become progressively more negative with increasing pressure because of the preferential diffusion of light radical species to the reaction zone, which tends to increase the laminar burning velocities of stretched flames at all fuel-equivalence ratios.

4) The present measurements of Markstein numbers and unstretched laminar burning velocities were in good agreement with earlier measurements where test conditions overlapped, even though the various other studies involved different experimental methods than the present study. In addition, predicted and measured unstretched laminar burning velocities were in reasonably good agreement for ethane/air flames and the extension of this mechanism for propane/air flames. On the other hand, predictions of unstretched laminar burning velocities of ethylene/air flames were less successful for reasons that are still not known.

Acknowledgments

This research was supported by National Science Foundation Grants CTS-9019813 and 9321959 under the technical management of M. J. Linevsky and F. Fisher. Support from the Peace Fellowship Program of Egypt for M. I. Hassan is also gratefully acknowledged. The authors also wish to thank F. N. Egolfopoulos for advice concerning the chemical reaction mechanisms considered during the present computations and especially for quantitative information about his extended C_3 kinetics.

References

[1]Kwon, S., Tseng, L.-K., and Faeth, G. M., "Laminar Burning Velocities and Transition to Unstable Flames in $H_2/O_2/N_2$ and $C_3H_8/O_2/N_2$ Mixtures," *Combustion and Flame*, Vol. 90, No. 3, 1992, pp. 230–246.

[2]Tseng, L.-K., Ismail, M. A., and Faeth, G. M., "Laminar Burning Velocities and Markstein Numbers of Hydrocarbon/Air Flames," *Combustion and Flame*, Vol. 95, No. 4, 1993, pp. 410–426.

[3]Aung, K. T., Tseng, L.-K., Ismail, M. A., and Faeth, G. M., "Response to Comment by S. C. Taylor and D. B. Smith on 'Laminar Burning Velocities and Markstein Numbers of Hydrocarbon/Air Flames'," *Combustion and Flame*, Vol. 102, No. 4, 1995, pp. 526–530.

[4]Aung, K. T., Hassan, M. I., and Faeth, G. M., "Flame/Stretch Interactions of Laminar Premixed Hydrogen/Air Flames at Normal Temperature and Pressure," *Combustion and Flame*, Vol. 109, No. 1, 1997, pp. 1–24.

[5]Aung, K. T., Hassan, M. I., and Faeth, G. M., "Effects of Pressure and Nitrogen Dilution on Flame/Stretch Interactions of Laminar Premixed $H_2/O_2/N_2$ Flames," *Combustion and Flame*, Vol. 112, No. 1, 1998, pp. 1–15.

[6]Hassan, M. I., Aung, K. T., and Faeth, G. M., "Properties of Laminar Premixed CO/H_2/Air Flames at Various Pressures," *Journal of Propulsion and Power*, Vol. 13, No. 2, 1997, pp. 239–245.

[7]Hassan, M. I., Aung, K. T., and Faeth, G. M., "Measured and Predicted Properties of Laminar Premixed Methane/Air Flames at Various Pressures," *Combustion and Flame* (to be published).

[8]Markstein, G. H., *Non-Steady Flame Propagation*, Pergamon, New York, 1964, p. 22.

[9]Clavin, P., "Dynamic Behavior of Premixed Flame Fronts in Laminar and Turbulent Flows," *Progress in Energy and Combustion Science*, Vol. 11, No. 1, 1985, pp. 1–59.

[10]Agnew, J. T., and Graiff, L. B., "The Pressure Dependence of Laminar Burning Velocity by the Spherical Bomb Method," *Combustion and Flame*, Vol. 5, No. 3, 1961, pp. 209–219.

[11]Dugger, G. L., and Dorothy, G. D., "Flame Velocities of Propane- and Ethylene-Oxygen-Nitrogen Mixtures," NACA RM E52J24, Jan. 1953.

[12]Gibbs, G. J., and Calcote, H. F., "Effect of Molecular Structure on Burning Velocity," *Journal of Chemical Engineering Data*, Vol. 4, No. 3, 1959, pp. 226–237.

[13]Manton, J., and Milliken, B. B., "Study of Pressure Dependence of Burning Velocities by the Spherical Vessel Method," *Proceedings of the Gas Dynamics Symposium on Aerothermochemistry*, Northwestern Univ., Evanston, IL, 1956, pp. 151–157.

[14]Metghalchi, M., and Keck, J. C., "Laminar Burning Velocity of Propane-Air Mixtures at High Temperature and Pressure," *Combustion and Flame*, Vol. 38, No. 2, 1980, pp. 143–154.

[15]Gilbert, M., "The Influence of Pressure on Flame Speed," *6th Symposium (International) on Combustion*, The Combustion Inst., Pittsburgh, PA, 1957, pp. 74–83.

[16]Palm-Leis, A., and Strehlow, R. A.. "On the Propagation of Turbulent Flames," *Combustion and Flame*, Vol. 13, No. 2, 1969, pp. 111–129.

[17]Egolfopoulos, F. N., Zhu, D. L., and Law, C. K., "Experimental and Numerical Determination of Flame Speeds: Mixture of C2-Hydrocarbons with Oxygen and Nitrogen," *23rd Symposium (International) on Combustion*, The Combustion Inst., Pittsburgh, PA, 1990, pp. 471–478.

[18]Wu, C. K., and Law, C. K., "On the Determination of Laminar Flame Speeds from Stretched Flames," *20th Symposium (International) on Combustion*, The Combustion Inst., Pittsburgh, PA, 1984, pp. 1941–1949.

[19]Yu, G., Law, C. K., and Wu, C. K., "Laminar Flame Speeds of Hydrocarbon + Air Mixtures with Hydrogen Addition," *Combustion and Flame*, Vol. 63, No. 3, 1986, pp. 339–347.

[20]Taylor, S. C., "Burning Velocity and Influence of Flame Stretch," Ph.D. Dissertation, University of Leeds, England, UK, 1991.

[21]Zhou, M., and Garner, C. P., "Direct Measurements of Burning Velocity of Propane-Air Using Particle Image Velocimetry," *Combustion and Flame*, Vol. 106, No. 3, 1996, pp. 363–367.

[22]Strehlow, R. A., and Savage, L. D., "The Concept of Flame Stretch," *Combustion and Flame*, Vol. 31, No. 2, 1978, pp. 209–211.

[23]Gordon, S., and McBride, B. J., "Computer Program for Calculation of Complex Chemical Equilibrium Compositions, Rocket Performance, Incident and Reflected Shocks, and Chapman-Jouguet Detonations," NASA SP-273, 1971.

[24]Reynolds, W. C., "The Element Potential Method for Chemical Equilibrium Analysis: Implementation in the Interactive Program STANJAN," Dept. of Mechanical Engineering, Stanford Univ., Stanford, CA, 1986.

[25]Kee, R. J., Dixon-Lewis, G., Warnatz, J., Coltrin, M. E., and Miller, J. A., "A FORTRAN Computer Code Package for the Evaluation of Gas-Phase, Multicomponent Transport Properties," Sandia National Labs., SAND86-8246, July 1992.

[26]Kee, R. J., Rupley, F. M., and Miller, J. A., "The CHEMKIN Thermodynamic Data Base," Sandia National Labs., SAND87-8215B, Oct. 1992.

[27]Kee, R. J., Rupley, F. M., and Miller, J. A., "CHEMKIN II: A Fortran Chemical Kinetics Package for the Analysis of Gas Phase Chemical Kinetics," Sandia National Labs., SAND89-8009B, Jan. 1993.

[28]Kee, R. J., Grcar, J. F., Smooke, M. D., and Miller, J. A., "A Fortran Program for Modeling Steady Laminar One-Dimensional Premixed Flames," Sandia National Labs., SAND85-8240, Jan. 1993.

[29]Grcar, J. F., Kee, R. J., Smooke, M. D., and Miller, J. A., "A Hybrid Newton/Time-Integration Procedure for the Solution of Steady, Laminar, One-Dimensional, Premixed Flames," *21st Symposium (International) on Combustion*, The Combustion Inst., Pittsburgh, PA, 1986, pp. 1773–1782.

[30]Peters, N., and Rogg, B., *Reduced Kinetic Mechanisms for Applications in Combustion Systems*, Springer–Verlag, Berlin, 1993, pp. 76–141.

[31]Warnatz, J., "Rate Coefficients in the C/H/O System," *Combustion Chemistry*, edited by W. C. Gardiner Jr., Springer–Verlag, New York, 1984, pp. 197–360.

[32]Westbrook, C. K., and Dryer, F. L., ''Simplified Reaction Mechanism for the Oxidation of Hydrocarbon Fuels in Flames,'' *Combustion Science and Technology*, Vol. 27, Nos. 1 and 2, 1981, pp. 31–43.

[33]Westbrook, C. K., and Dryer, F. L., ''Chemical Reaction Modeling of Hydrocarbon Combustion,'' *Combustion Science and Technology*, Vol. 40, Nos. 1–4, 1984, pp. 31–43.

[34]Linstedt, R. P., and Maurice, L. Q., ''Detailed Kinetic Modeling of *n*-Heptane Combustion,'' *Combustion Science and Technology*, Vol. 107, Nos. 4–6, 1995, pp. 317–353.

[35]Law, C. K., ''Dynamics of Stretched Flames,'' *22nd Symposium (International) on Combustion*, The Combustion Inst., Pittsburgh, PA, 1988, pp. 1381–1402.

[36]Padley, P. J., and Sugden, T. M., ''Chemiluminescence and Radical Recombination in Hydrogen Flames,'' *7th Symposium (International) on Combustion*, The Combustion Inst., Pittsburgh, PA, 1958, pp. 235–242.